DYNAMIC TESTING OF MATERIALS USING SHPB AND DICT ON TYPICAL AND MINIATURIZED SPECIMENS – NUMERICAL MODELLING AND EXPERIMENT

Zbigniew L. Kowalewski, Zdzisław Nowak and Ryszard B. Pęcherski

**Institute of Fundamental Technological Research,
Polish Academy of Sciences
Pawińskiego 5B Street, 02-106 Warsaw, Poland
zkowalew@ippt.pan.pl, znowak@ ippt.pan.pl, rpecher @ippt.pan.pl**

Keywords: Dynamic tests, Direct Impact Compression Test, Hopkinson bar, punching effect

Abstract. *The results of experimental and numerical investigations concerning the influence of strain rate on mechanical properties of pure tantalum and VP159 high nitrogen austenitic steel are presented. Experiments were carried out using Split Hopkinson Pressure Bar (SHPB) and Direct Impact Compression Test (DICT) technique. The Perzyna elasto-viscoplasticity theory was applied to predict the dynamic compression yield strength of the tantalum at strain rates from 1.0×10^{-3} s^{-1} to 0.5×10^{6} s^{-1}. In the case of the VP159 high nitrogen austenitic steel the experimental results were used to calibrate the Rusinek-Klepaczko model.*

There are still no sufficient data on the flow stress at higher strain rates than $1.0 \times 10^{5} s^{-1}$, in particular for large strains. The experimental identification of material parameters required for constitutive modelling are not sufficiently reported. This paper is an attempt to supplement our knowledge in this area.

The impact resistance of material in question is analysed numerically with use of ABAQUS/Explicit finite element program. The Huber-Mises-Hencky yield criterion and Perzyna viscoplasticity model with adiabatic conditions are used.

1 INTRODUCTION

In engineering practice the examples of high strain rate loading are high velocity impact, high velocity machining, and high energy rate forming. In order to predict and control behaviour of materials used under such extreme loading conditions, the mechanical deformation behaviour of materials should be known. It is well known that the mechanical behaviour of metal depends on the applied strain rate. The Split Hopkinson Pressure Bar (SHPB) or Kolsky apparatus is widely used for the study of mechanical behaviour of materials at high strain rates up to 1.0×10^{3} s^{-1}. SHPB apparatus works based on wave propagation theory in elastic bars. Some details regarding SHPB technique are presented in [1–5]. In order to reach higher strain rates than 1.0×10^{3} s^{-1}, Dharan and Hauser (1970) [6] introduced a modification of the SHPB concept by eliminating the incident bar. Thus, application of the direct impact of a striker onto a small disk or prismatic specimen supported by the transmitter bar enabled to reach strain rates up to 0.5×10^{6} s^{-1}. Such modification can be defined as the Direct Impact Compression Test (DICT) [7, 8].

Although a simplified theory of the DICT has been developed some time ago by Dharan and Hauser

[6] the some new points of view on the DICT measurement side have already been added by Klepaczko [9]. From the direct impact experiment, the following quantities are determined: the impact velocity V_0, the transmitted elastic wave $\sigma(t)$ and the specimen displacement $\Delta U = U_A(t) - U_B(t)$, where U_A is the displacement of the striker/specimen interface and U_B is the displacement of the specimen/transmitter bar interface. The average velocity of the specimen compression is $V = V_A - V_B = d\Delta U(t)/dt$. Having recorded all of those quantities, the specimen strain $\varepsilon(t)$, the strain rate $\dot{\varepsilon}(t)$, and the mean stress $\sigma(t)$, all as a function of time, can be calculated by application of the DICT theory.

In order to ensure a valid numerical simulation of the high-strain-rate effects a constitutive model describing the dynamic mechanical behaviour of materials at high strain rate, high temperature, and large plastic strain is needed. In literature, a large number of constitutive models have been proposed to describe the dynamic deformation behaviour of metals. The parameters used in constitutive rate dependent plasticity models are generally determined from experiment such as the SHPB test and Taylor impact test. Constitutive models can be sorted into two groups: physical and phenomenological. In description of the relation between the flow stress and plastic strain, the physical models consider associated mechanisms such as thermally activated dislocation movement. They are very useful to understand the mechanisms associated with the dynamic deformation. Among the many physically based constitutive models developed in 1960's, the Perzyna (PP) model [10] has been one of the most widely utilized.

Rusinek and Klepaczko [11] have proposed a model (RK) to cover wide ranges of strain rate and reflecting the temperature sensitivity on the flow stress. The RK model reasonably describes the yield stress and the strain-hardening behaviour of the materials deforming at a low and intermediate strain rates. It was used in this paper to describe the experimental data for steel.

The PP mechanical threshold stress model was introduced with the idea that plastic deformation is controlled by the thermally activated interactions of dislocations with obstacles. In the PP model, in addition to the thermally activated interactions that have dominant effect in a low strain rate regime, the dislocation drag mechanism is introduced to cover high strain rates over 10^7 s^{-1}.

In this paper, we have applied the modification of the Perzyna model by replacing the Ludwik strain-hardening-related term $(A+B\varepsilon^n)$ with Voce hardening law. It successfully describes the flow stress and direct impact test results of tantalum in wide range of strain rate and strain.

2 EXPERIMENTAL DETAILS

2.1 Materials

Commercially pure tantalum and X4CrMnN16-12 (VP159) austenitic high-nitrogen steel were used in the present study. The tantalum had a grain size of about 85 μm. Chemical composition of tantalum is as follows: 20.3–20.7% C; 31.9–33.9% Fe; 3.9–4.9% Mo; 6–8% Si; Pmax−0.05; Smax−0.05, while VP159 steel: 0.04% C; 0.30% Si; 16.5 % Cr; 12% Mn; 0.61 N and rest Fe.

2.2 Details of testing parameters and equipment

Compression tests were carried out on both materials at strain rates ranging from quasi-static to dynamic at room temperature 296 K. Strain rates of 10^{-3} s^{-1} to 10^0 s^{-1} and room temperature 296 K were achieved in a servo-hydraulic Instron testing machine, whereas strain rates of 10^3 s^{-1} and 0.5×10^6 s^{-1} were achieved using the SHPB and miniaturized DICT, respectively.
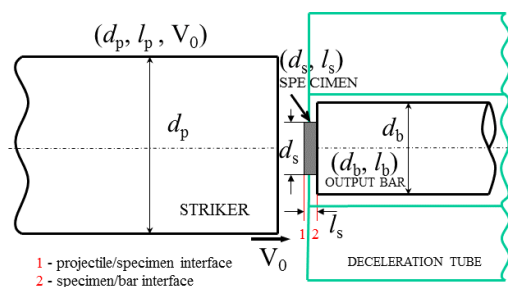

Figure 1: The schematic arrangement of the Direct Impact Compression Test.
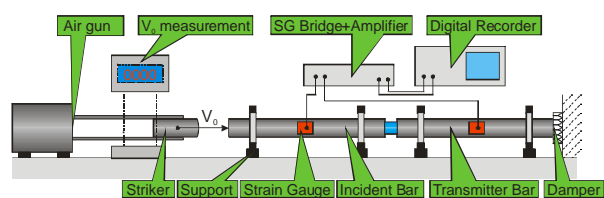

Figure 2: Scheme of the Split Hopkinson Pressure Bar used in the tests

The main details of the miniaturized DICT are shown in Fig. 1, whereas general view of the SHPB in Fig. 2. In the miniaturized DICT the decelerator tube is used in which a small output bar with miniature gages is inserted. The decelerator tube is mounted in supports slightly ahead of the output bar with possibility to change the distance between them and such configuration permits programming of different plastic deformations of specimens. In the literature, the flow stress of commercially pure tantalum has been studied at strain rates ranging from quasi-static 1.0×10^{-3} s^{-1} to dynamic 1.0×10^{4} s^{-1}, temperatures from $-200\ ^{0}$C to 700^{0}C (cf. Nemat-Nasser and Isaacs [11], and strains up to 0.8-1.0, cf. Kim and Shin [12]). It has to be mentioned however, that still the number of experimental data on the flow stress at higher strain rates than 1.0×10^{5} 1/s and large range of strain is far from the requirements for optimal validation of constitutive models.

3 CONSTITUTIVE RELATIONS

Among many constitutive relations the most advanced are those that include strain hardening and also strain rate and temperature sensitivities of flow stress. In the present work the Perzyna and Rusinek-Klepaczko are taken into account.

3.1 The thermo-elasto-viscoplastic relations

We propose to introduce some simplification of the constitutive model developed by Perzyna [13] by assuming that the internal state variable vector $\mu = (\in^{p}, \boldsymbol{\xi})$ consists of two scalars and one tensor, where $\in^{p}$ denotes the equivalent viscoplastic deformation and $\boldsymbol{\xi}$ is the microdamage second order tensor, with the physical interpretation that $(\boldsymbol{\xi} : \boldsymbol{\xi})^{1/2} = \xi$ defines the volume fraction porosity. The equivalent inelastic deformation $\in^{p}$ describes the dissipation effects generated by viscoplastic flow phenomena.

The plastic potential function in the form $f = f(J_{1}, J_{2}, \vartheta, \boldsymbol{\mu})$ is postulated, where J_{1}, J_{2} denote the first two invariants of the Kirchhoff stress tensor $\boldsymbol{\tau}$ and ϑ is absolute temperature. The evolution equations are assumed as follows

$$\mathbf{d}^{p} = \Lambda \mathbf{P}, \ \mathrm{L}_{\upsilon}\boldsymbol{\xi} = \Xi \tag{1}$$

where

$$\Lambda = \frac{1}{T_{rel}} \langle \Phi(\frac{f}{\kappa} - 1) \rangle, \quad \mathbf{P} = \frac{\partial f}{\partial \boldsymbol{\tau}}\bigg|_{\xi=const} \left(\left\| \frac{\partial f}{\partial \boldsymbol{\tau}} \right\| \right)^{-1}, \tag{2}$$

$\mathbf{d}^{p}$ denotes the rate of inelastic deformation tensor, T_{rel} denotes the relaxation time for mechanical disturbances, the isotropic work-hardening-softening function $\kappa = \hat{\kappa}(\in^{p}, \vartheta, \boldsymbol{\xi})$, Φ is the empirical overstress function, the bracket $\langle \cdot \rangle$ defines the ramp function, L_{υ} denotes the Lie derivative and Ξ denotes the evolution function which has to be determined.

This constitutive relation has been implemented into ABAQUS/Explicit using the stress integration scheme proposed by Perzyna [13]. The main idea in Perzyna constitutive relation is to accomplish in one model the description of behaviour of the material for the entire range of strain rates. To achieve this aim the empirical overstress function Φ has been introduced and the equivalent plastic strain rate has been postulated in the following form [13]

$$\dot{\bar{\varepsilon}}^{p} = \frac{1}{T_{rel}(\dot{\bar{\varepsilon}}^{p})} \left\langle \Phi\left[\frac{\sigma_{eq}}{\sigma_{y}(\bar{\varepsilon}^{p}, T)} - 1 \right] \right\rangle \tag{3}$$

where T_{rel} is the relaxation time for mechanical disturbances, $\langle \bullet \rangle$ denotes the Macauley bracket and $\sigma_{y}(\bar{\varepsilon}^{p}, T)$ is the static yield stress function. The static yield stress function depends on the plastic strain $\bar{\varepsilon}^{p}$ and temperature T. The empirical overstress function Φ may be determined basing on the available experimental results.

By developing the expression showed above, it is possible to achieve an explicit definition for the equivalent Huber-Misses stress $\bar{\sigma}$. The tantalum material is modelled as elastic-viscoplastic with thermal softening. In the present paper the formulation used is described in the following way

$$\overline{\sigma}(\overline{\varepsilon}^p, \dot{\overline{\varepsilon}}^p, T) = \left[(A + B(1 - \exp(-C\overline{\varepsilon}^p)) \right] \left[1 + \left(T_{rel}(\dot{\overline{\varepsilon}}^p) \cdot \dot{\overline{\varepsilon}}^p \right)^D \right] (1 - \Theta^m) \tag{4}$$

where the exponential form of the overstress function Φ is assumed [13].

It is a multiplicative law which shows some similarities with the Johnson-Cook formulation [14]. In fact those terms corresponding to strain hardening *(first bracket in Eq. 4)* and temperature sensitivity *(third bracket in Eq. 4)* are defined in the same way. Thus, *A* is a material constant related to the quasi-static yield stress, *B* is the modulus of strain hardening, *n* is the strain hardening exponent, *m* defines the temperature sensitivity and Θ is the modified temperature given by:

$$\Theta = \frac{T - T_0}{T_m - T_0} \tag{5}$$

where T_0 is the reference temperature and T_m is the melting temperature.

Contrary to the **JC** formulation, in the case of Perzyna model [13] the strain rate sensitivity of the material (*second bracket in Eq. 4*) is defined taking into account the physical assumptions on rate dependent material behaviour. In such definition *D* is the strain rate sensitivity exponent, which is a material constant and it can be determined using experimental data. Moreover, it is assumed that the relaxation time $T_{rel}(\dot{\overline{\varepsilon}}^p)$ controls the viscoplastic flow in the entire range of strain rate changes. In classical Perzyna model it is generally assumed as constant value. However, in real case it has to be a function of the rate of inelastic deformation $\dot{\overline{\varepsilon}}^p$ and may be determined based on experimental data.

The following constant values have been found obtaining the best possible fitting with experimental results for tantalum [8, 15], Table 1.

A (MPa)	B (MPa)	C (-)	T_{rel} (s)	$\dot{\varepsilon}_0$ (s^{-1})	D (-)	T_0 (K)	m (-)	T_m(K)
156	256	5.0	4.545E-02	0.001	0.2	296	0.25	3150

Table 1: Constants determined for tantalum for Perzyna model with Voce hardening law

In the case of adiabatic conditions of deformation the constitutive relations considered are combined with the energy balance principle. Such relation allows for an approximation of the thermal softening of the material via the adiabatic heating

$$T_{adia} = T_0 + \Delta T_{adia} \tag{6}$$

$$\Delta T_{adia} = \frac{\chi}{\rho C_p} \int_{\varepsilon^e}^{\overline{\varepsilon}^p} \sigma(\xi, \dot{\overline{\varepsilon}}^p, T) d\xi \tag{7}$$

where χ is the Taylor-Quinney coefficient, ρ is the material density and C_p is the specific heat at constant pressure. Transition from isothermal to adiabatic conditions is assumed at $\dot{\overline{\varepsilon}}^p = 10 s^{-1}$, in agreement with experimental observations and numerical estimations for steels [16, 17, 18].

For temperature sensitivity including adiabatic heating under dynamic compression, Eq. (4), the additional constants may be used (Table 1).

Figure 4 shows comparison of the Perzyna model (solid lines) with the experimental flow stress data (symbols ◊) of pure tantalum with respect to logarithmic strain rate at 296 K and varying strains ε=0.02, 0.1 and 0.3. The hardening law Eq. (4) is specified for: A = 29.8 MPa, B = 314.8 MPa, C = 6.90, D = 0.0124, m = 0.25. There is an increase in dynamic yield strength of tantalum at high strain rate loading comparing with that one corresponding to the quasi-static test. In the range of the strain rates considered, the strength magnification factor is up to 3.0 for pure tantalum. A good correlation between the experimental data and the Perzyna overstress model predictions for strain rates up to 0.5x10^6 s^{-1}
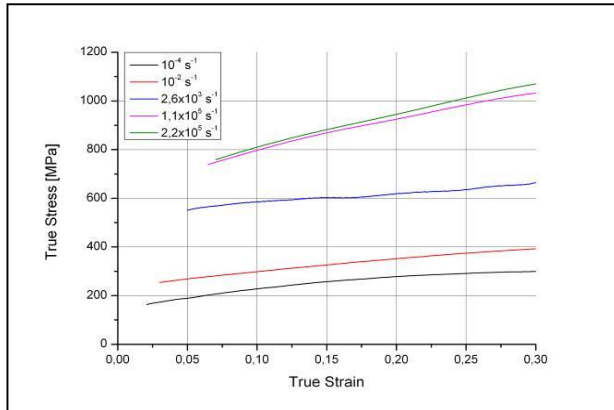
can by clearly observed.
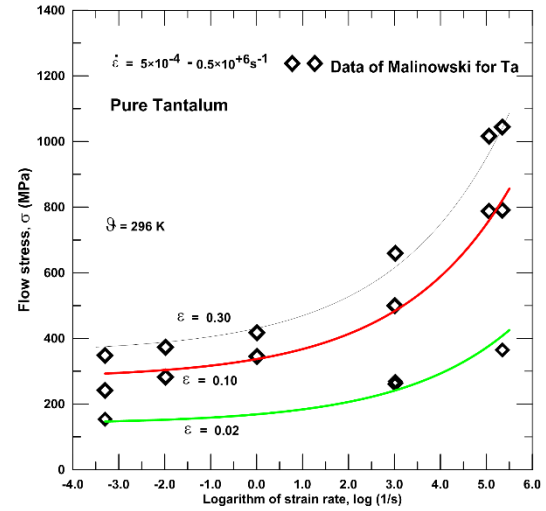

Figure 3: Dynamic stress-strain characteristics for tantalum.

Figure 4: Comparison of the Perzyna model (solid lines) with the experimental data (symbols ◊) of pure tantalum with respect to logarithmic strain rate at 296 K and varying strains ε=0.02, 0.1 and 0.3.

3.2 Rusinek-Klepaczko model

The model proposed by Rusinek and Klepaczko (RK) [19] often presents a much more precise description of the mechanical properties variation of materials in question, particularly under dynamic loads, than others available in the contemporary papers. According to the RK model's assumptions, the equivalent stress can be decomposed into: internal stress σ_μ, effective stress σ^*, and viscous-drag stress $\overline{\sigma}_d$. The relation takes into account the thermal softening of a material caused by a change in the Young's modulus variation and the dependencies between internal stress and strain, strain rate and temperature. The effective stress presented in the equation considers the coupled relationships between strain rate and temperature. The equation takes the following general form [19]:

$$\overline{\sigma}(\overline{\varepsilon}^p,\dot{\overline{\varepsilon}}^p,T) = \frac{E(T)}{E_0}\left[\sigma_\mu(\overline{\varepsilon}^p,\dot{\overline{\varepsilon}}^p,T) + \sigma^*(\dot{\overline{\varepsilon}}^p,T)\right] + \overline{\sigma}_d(\dot{\overline{\varepsilon}}^p,T) \tag{8}$$

where $\overline{\sigma}(\overline{\varepsilon}^p,\dot{\overline{\varepsilon}}^p,T)$ - overall flow stress, $\overline{\sigma}_\mu(\overline{\varepsilon}^p,\dot{\overline{\varepsilon}}^p,T)$ - internal stress component, $\overline{\sigma^*}(\dot{\overline{\varepsilon}}^p,T)$ - effective stress component, $\overline{\sigma}_d(\dot{\overline{\varepsilon}}^p,T)$ - drag stress component, E(T) - temperature dependence of the Young's modulus, E_0 - Young's modulus at T=0K, T – temperature, $\dot{\overline{\varepsilon}}^p$ - strain rate, $\overline{\varepsilon}^p$ - inelastic strain.

The results of the RK model for the steel tested [17] are presented in Fig. 5. As it is seen, quite reasonable fit was achieved.
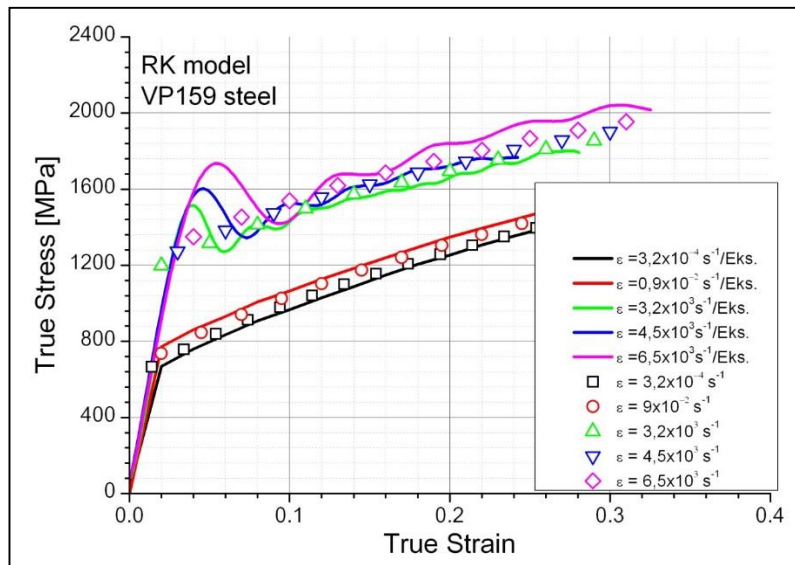
Figure 5: Comparison of the experimental data and results calculated using the RK model

4   NUMERICAL CALCULATIONS

The mechanical properties of the tantalum used in the simulation are as follows: Young's modulus 186 GPa, Poisson ratio – 0.34, bulk modules - 194 GPa, shear modules - 69.4 GPa, initial compression yield stress – 136 MPa, melting point (K) – 3269, and density – 16600 kg/m^3. The material constants for striker and output bar Marval steel used in the calculation are as follows: Young's modulus 206 GPa, Poisson ratio – 0.32, and density – 8000 kg/m^3.

The impact resistance of tantalum is analysed numerically using ABAQUS/Explicit finite element program. The numerical model contains four main parts: striker, specimen, deceleration tube and output bar. In numerical simulations the specimen is supported by a output bar and is impacted by a striker bar moving one with an imposed velocity. Bottom displacements of output bar and deceleration tube in the impact direction are fixed. Both bars in contact with specimen are chosen as an elastic bodies with finite friction. Penalty type of contact with friction coefficient for specimen/striker (Ta/steel) and for specimen/ output bar (steel/Ta) equal 0.05 are assumed. Simulation leads to plastic strain and strain rates in the range from 1.0 x10^{-3} s^{-1} to 0.5 x10^6 s^{-1}. Linear theory of elasticity, the Huber-Mises-Hencky yield criterion, Perzyna viscoplasticity with adiabatic conditions are used. The equation of adiabatic heat conduction with internal sources applicable to dynamic plasticity is applied with Taylor–Quinney coefficient χ=0.8. The finite elements model consists: for the striker+bar+tube - 31800 nodes and 36850 elements, and for the specimen - 1881 nodes and 1500 elements, Fig. 6. All elements are of the type C3D8R (ABAQUS).
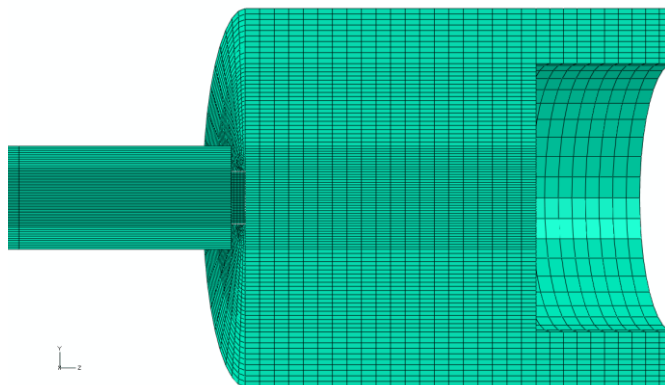

Figure 6: The mesh of the transmitted bar, specimen and striker

Strain rate distribution for specimen tested using DICT technique for t=1.0 and 4.1 µs are presented in Figs 7 and 8, respectively.
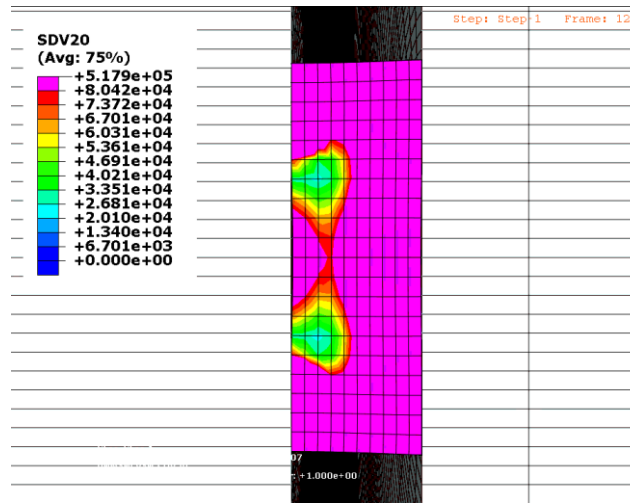

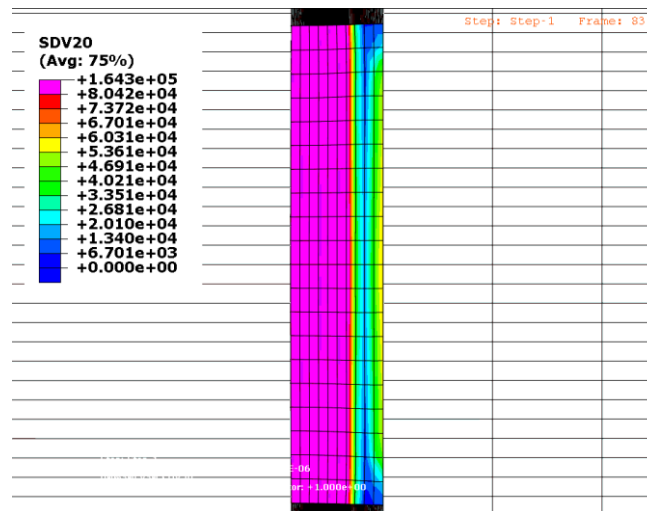Figure 7: Strain rate distribution in specimen along compression axis for t=1µs

Figure 8: Strain rate distribution in specimen along compression axis for t=4.1µs

4.1 Punching effect

Phenomena related to the punching induce an error estimation concerning the macroscopic longitudinal strain imposed on the specimen. As it is shown in Fig. 9, during dynamic loading the bar is deformed elastically inducing a local displacement U_2(r, t). As it was reported in [20], it is necessary to include this additional displacement in the definition of the real length change of the specimen. However, it is not possible to measure this punching displacement in a precise way with a known experimental setup measurement. In this section, the displacement induced by punching effect U_2(r, t) is analyzed to estimate how it may disturb the macroscopic average strain ε of the specimen using the displacement measurement of the DICT. The correction that takes the punching displacement U_2(r, t) into account was reported in [20]. The correction proposed in [20] to define the specimen length change, is based on the estimation of the striker displacement U_2 associated to the punching effect. The punching displacement U_2(r, t) is generally not included in estimation of the average strain ε of the specimen. This effect is mainly related to the geometry as the friction effect discussed previously but also to the yield stress. Higher the strength or yield stress of the material strengthens the punching effect. Using numerical simulations, the displacement related to the punching effect was computed. Simulations of the DICT was prepared for the different sizes of test specimens. It is clear from this analysis that, the

180

punching effect is larger for higher impact velocity. Therefore, the Young modulus measured in experiment $E_{measured}$ will be lower in comparison to the theoretical value $E_{theoretical}$. However, it is possible to improve the measurement to correct stiffness using the following formula for correction of the punching displacement:

$$\varepsilon_{corrected}(t) = \varepsilon_{measured}(t) - \sigma_{measured}(t)\left[\frac{E_{theoretical} - E_{measured}}{E_{theoretical}E_{measured}}\right] \qquad (9)$$
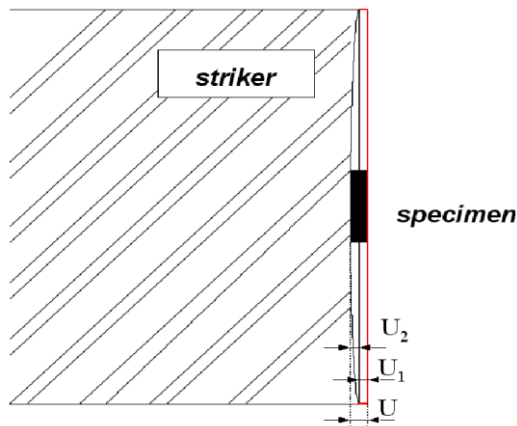

Figure 9: Schematic description of the punching effect during dynamic compression using DICT
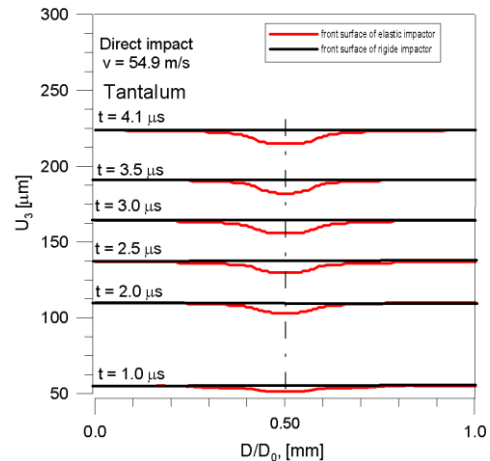

Figure 10: The punching effect during dynamic compression using DICT with V_0 =54.95 m/s results for tantalum. Elastic displacement U_3 distribution on striker front surface in time t=1.0 - 4.1μs.
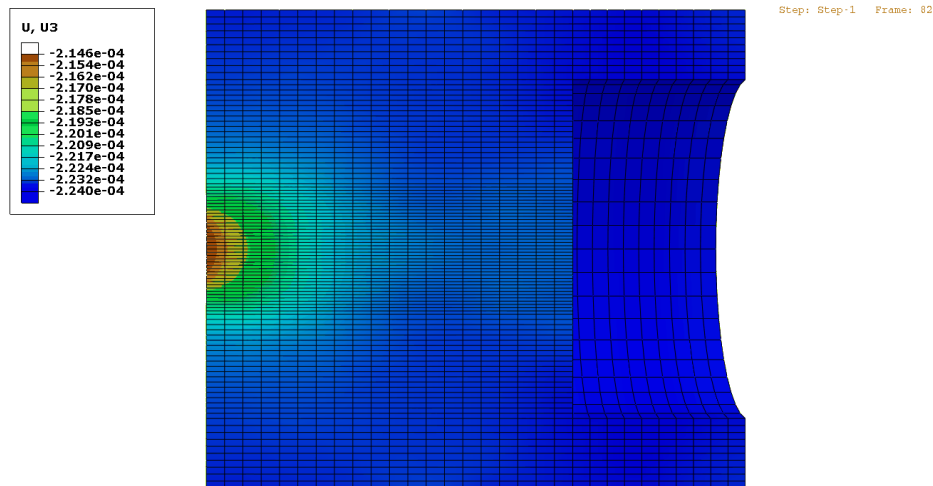

Figure 11: Contour plot of elastic displacement U_3 distribution in volume of striker for t=4.1μs in DICT with V_0 =54.95 m/s, results for tantalum.

The strain level $\varepsilon_{corrected}$ for an imposed stress intensity is changed. This effect is particularly important for brittle materials that fail at very small strain. In the case of ductile material the punching effect is of secondary importance since the failure strain level is larger than 10%. The results show that the measured Young's modulus $E_{measured}$ using elastic wave theory underestimates the theoretical values. Therefore the modulus correction, using Eq. (9), shifts the measured results closer to the theoretical one $E_{theoretical}$. However, Eq. (9) is not valid for visco-elastic material and a correction must be used.

In addition, the punching displacement is reported by the following curves for impact velocity 54.95

m/s . Several measurement points are used with *r* being the axis of the striker. The numerical result presented in Fig. 10 and Fig. 11 proofs that the punching effect does not change significantly the macroscopic strain level at low and high impact velocity. However, for brittle material as ceramics, this effect must be taken into account since the maximum strain level is close to $\varepsilon=0.01$.

5 STRAIN RATE SENSITIVITY OF MATERIALS

The final set of quasi-static and dynamic $\sigma(\varepsilon)$ curves for tantalum and steel is shown in Figs. 3 and 5, respectively. The range of strain rate is nine decimal orders, that is from 10^{-4} s^{-1} to $2,2\times10^5$ s^{-1}. All curves are in true coordinates and corrected to isothermal conditions. The effect of strain rate on the flow stress is shown in Figs. 12 and 13 for three levels of strain for tantalum and steel, respectively. The rate sensitivity $\beta=(\partial\sigma/\partial\log\dot{\varepsilon})_{\varepsilon}$ for tantalum shows two ranges, at lower strains $\beta \approx 46$ MPa and $\beta \approx 260$ MPa above the strain rate threshold $\dot{\varepsilon}_C \approx 1000$ s^{-1}. Such result suggests existence of two thermally activated dislocation micro-mechanisms of plastic deformation in those two ranges of strain rate [21]. Similar result was obtained for steel, Fig.13. It can be seen that strain rate sensitivity for tantalum is much greater than for VP159 steel obtained. For both materials it changes around 5×10^3s^{-1}.
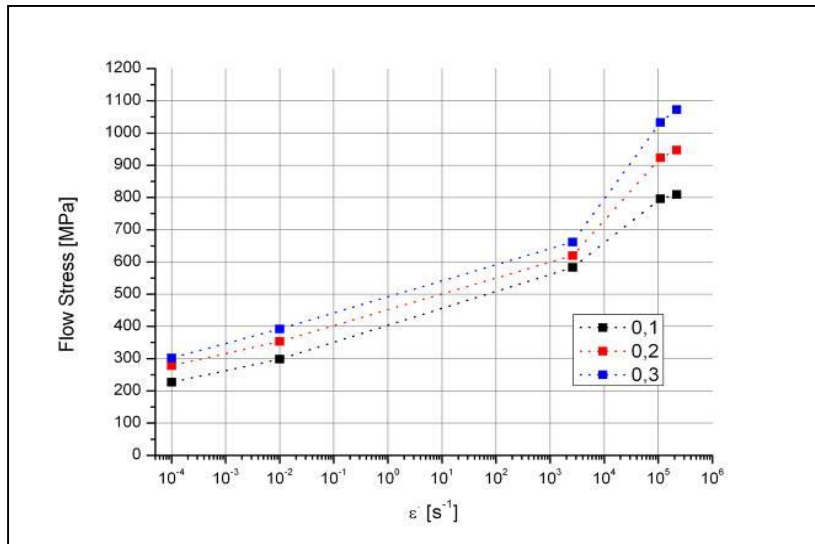

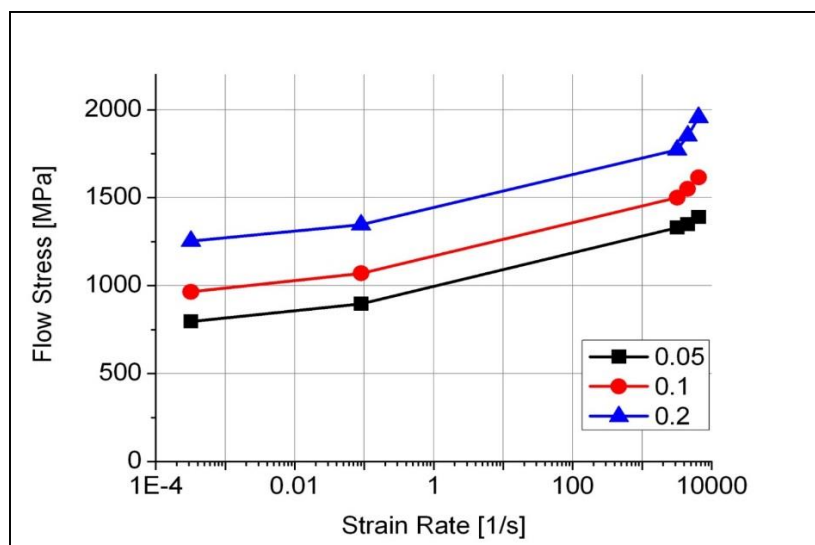Figure 12: Rate sensitivity of the tantalum at three levels of true strain

Figure 13: Rate sensitivity of the steel at three levels of true strain

6 CONCLUSIONS

Dynamic hardening observed for tantalum is stronger than that for VP159 steel observed. In comparison to the quasi-static test for the tantalum and steel a significant increase of the yield strength was obtained at high strain rate investigations. The strength magnification factor was up to 3.0 in the range of the strain rates considered. Strain rate sensitivity for tantalum is much greater than for VP159 steel obtained. For both materials it changes around $5 \times 10^3 \, \text{s}^{-1}$

A good correlation between the experimental data and the Perzyna overstress model predictions can by clearly observed for strain rates up to $0.5 \times 10^6 \, \text{s}^{-1}$.

REFERENCES

[1]   H. Kolsky, *An Investigation of the Mechanical Properties of Materials at Very High Rates of Loading*, Proc. Phys. Soc. London, Sect. B, 62, pp. 676–700 (1949)

[2]   U.S. Lindholm, *Some Experiments with the Split Hopkinson Pressure Bar*, J. Mech. Phys. Solids, 12 (5), 317 (1964).

[3]   E.D.H. Davies, S.C. Hunter, *The Dynamic Compression Testing of Solids by the Method of the Split Hopkins Pressure Bar*, J. Mech. Phys. Solids, 11, 155 (1963).

[4]   M.A. Meyers, 1994, *Dynamic Behavior of Materials*, Wiley, New York, pp. 23–65 (1994).

[5]   B.A.Gama, S.L. Lopatnikov, and J.W., Jr., Gillespie, *Hopkinson Bar Experimental Technique, A Critical Review*, Appl. Mech. Rev., 57, pp. 223–249 (2004).

[6]   C.K.M. Dharan, F.E. Hauser, *Determination of Stress – Strain Characteristic at Very High Strain Rates, Experimental Mechanics*, 10, 370 (1970).

[7]   D. Jia, K.T Ramesh, *A Rigorous Assessment of the Benefits of Miniaturization in the Kolsky Bar System*, Experimental Mechanics, 44, 445 (2004).

[8]   J.Z. Malinowski, J.R. Klepaczko, Z.L. Kowalewski*, Miniaturized compression test at very high strain rates by direct impact*, Experimental Mechanics, 47, 451-463 (2007).

[9]   J.R. Klepaczko, *Advanced Experimental Techniques in Materials Testing, in: New Experimental Methods in Material Dynamics and Impact*, Inst. Fund. Technological Res., Polish Academy of Sciences, Warsaw, 223 (2002).

[10]   P. Perzyna, *Fundamental problems in viscoplasticity*, Adv. Appl. Mech., 9, 343–377 (1966).

[11]   S. Nemat-Nasser, J. Isaacs, *Direct measurement of isothermal flow stress of metals at elevated temperatures and high strain rates with application to Ta and Ta–W alloys*, Acta Metall., pp. 907-909 (1997).

[12]   J.B. Kim and H. Shin, *Comparison of plasticity models for tantalum and a modification of the PTW model for wide ranges of strain, strain rate, and temperature*, Int. Journal of Impact Engineering, pp. 746-753 (2009).

[13]   P. Perzyna, *The thermodynamical theory of elasto-viscoplasticity for description of nanocrystalline metals*, Engng. Trans., 58, 1-2, 15-74 (2010).

[14]   G.R. Johnson, W.H. Cook, *A constitutive model and data for metals subjected to large strains, high strain rates and high temperatures*, Proceedings of Seventh International Symposium on Ballistics, The Hague, The Netherlands, pp. 541-547 (1983).

[15]   K.E.Duprey, R.J. Clifton, *Dynamic constitutive response of tantalum at high strain rate*, The tenth American Physical Society topical conference on shock compression of condensed matter. AIP Conference Proceedings, Volume 429, pp. 475-478 (1998).

[16]   O. Oussouaddi, J.R. Klepaczko, *Analysis of transition between the isothermal and adiabatic deformation in the case of torsion of a tube*, Journal de Physique IV, **1**, 323-334 (1991).

[17]   W. Moćko, Z.L. Kowalewski, *Perforation test as an accuracy evaluation tool for a constitutive model of austenitic steel*, Archives of Metallurgy and Materials, 58, No.4, 1105-1110 (2013).

[18]   P. Larour, A. Rusinek, J.R. Klepaczko, W. Bleck, *Effects of Strain Rate and Identification of Material Constants for Three Automotive Steels*, Steel Research International 78(4):348-358 (2007).

[19]   A. Rusinek, J.R. Klepaczko, *Shear testing of sheet steel at wide range of strain rates and a constitutive relation with strain-rate and temperature dependence of the flow stress*, International Journal of Plasticity, 1, 17, 87-115 (2001).

[20]   K. Safa, G. Gary, *Displacement correction for punching at a dynamically loaded bar end*, I. J. Impact Eng., 37, 371-384 (2010).

[21]   J.R. Klepaczko, J. Duffy*, Strain Rate History Effects in Body-Center-Cubic Metals, ASTM-STP 765*, 251 (1982).